ZEUS-prel-06-013

Submitted to the
XXXIII International Conference on High Energy Physics
July 26 - August 2, 2006, Moscow, Russia

Abstract: **Session: QCD hard interactions, Heavy quark physics**

Measurement of beauty production in deep inelastic scattering at HERA II

ZEUS Collaboration

Abstract

Beauty production in deep inelastic scattering with events in which a muon and a jet are observed in the final state has been measured with the ZEUS detector at HERA II using an integrated luminosity of $39\,\mathrm{pb}^{-1}$. The fraction of beauty quarks in the data was determined using the distribution of the transverse momentum of the muon relative to the jet. The cross section for beauty production was measured in the kinematic range $Q^2 > 4\,\mathrm{GeV}^2$, $0.05 < y < 0.7$ and requiring a muon with $p_T^{\mu} > 1.5\,\mathrm{GeV}$ and $\eta^{\mu} > -1.6$ and a jet with $E_T^{\mathrm{jet}} > 5\,\mathrm{GeV}$ and $-2 < \eta^{\mathrm{jet}} < 2.5$. Differential cross sections in Q^2, p_T^{μ}, η^{μ}, p_T^{jet} and η^{jet} are compared to theoretical predictions. Double differential cross sections are also measured and compared to theory.

1 Introduction

QCD calculations are expected to be reliable if a hard scale is present in the process. In heavy quark production a hard scale is provided by the quark mass that is larger than the energy scale at which quarks are confined into hadrons, $\Lambda \sim 250\,\text{MeV}$. While QCD calculations provide an acceptable description of charm quark production ($m_c \sim 1.3\,\text{GeV}$), it is expected that the description is even more precise for the production of the heavier beauty quark ($m_b \sim 4.5\,\text{GeV}$). This process has been measured in different experiments at different accelerators. In early experiments at the Tevatron $p\bar{p}$ collider (CDF [1] and DØ [2]) the production rate was significantly higher than predicted. After recent improvements of the experiments and the theoretical calculations, data and QCD calculations are in good agreement [3].

At the HERA ep collider experiments (H1 [4–7] and ZEUS [8–10]), discrepancies between data and QCD calculations are found only in specific regions of phase space such as at low transverse momentum p_t^μ and large pseudorapidity η^μ of a muon from semi-leptonic beauty decay.

This paper reports the first ZEUS measurement at HERA II of beauty production in deep inelastic scattering (DIS), in the reaction with at least one jet and one muon in the final state:

$$e^+\, p \to e^+\, b\bar{b}\, X \to e^+\, \mu\, \text{jet}\, X'.$$

The analysis described here measures in an extended kinematic region compared to the previous analysis of HERA I data [9] and uses a combination of multiple detector components for muon identification. This allows a lower muon transverse momentum threshold and a higher detection efficiency to investigate these regions of phase space further.

Due to the large b-quark mass, muons from semi-leptonic b decays usually have high values of p_T^{rel}, the transverse momentum of the muon with respect to the axis of the closest jet. For muons from charm decays and in events induced by light quarks, where some of the produced hadrons are misidentified as muons, the p_T^{rel} values are lower. Therefore, the fraction of events from b decays in the data sample can be extracted by fitting the p_T^{rel} distribution of the data to Monte Carlo (MC) simulations of the processes producing beauty, charm and light quarks. In this analysis a visible cross section, $\sigma_{b\bar{b}}$ and differential cross sections as a function of the photon virtuality Q^2, the transverse momentum of the muon, p_T^μ and its pseudorapidity[1] η^μ as well as the transverse momentum of the jet, p_T^{jet} and η^{jet} are compared to the leading order (LO) plus parton shower (PS) MC predictions and next-to-leading-order (NLO) QCD calculations. Furthermore the main ingredient for

[1] The pseudorapidity is defined as $\eta = -\ln\left(\tan\frac{\theta}{2}\right)$, where the polar angle, θ, is measured with respect to the proton beam direction.

the determination of the beauty contribution to the proton structure function F_2, i.e. double differential cross sections $d^2\sigma/dQ^2dx$, are measured.

2 Data sample and selection

The data used in this measurement were collected during the 2003−2004 HERA II running period, where a proton beam of 920 GeV collided with a positron beam of 27.5 GeV, corresponding to an integrated luminosity 39.1 pb^{-1}. A detailed description of the ZEUS detector can be found elsewhere [11]. A brief outline of the components that are most relevant for this analysis is given below. The reconstruction of observables characterising the event topology and kinematic variables was based on combined information from the compensating uranium scintillator calorimeter (CAL) [12], the central tracking detector (CTD) [13], the silicon micro vertex detector (MVD) [14], the forward, barrel and rear muon chambers (FMUON, BMUON and RMUON) [11], the backing calorimeter (BAC) [15] and the luminosity monitor [16]. Events were selected by requiring the presence of at least one muon in the final state and at least one jet. The final sample was selected in four steps: 1) inclusive DIS event selection, 2) muon finding, 3) jet finding and 4) muon-jet association.

1. DIS events were selected by requiring a well reconstructed outgoing positron with energy greater than 10 GeV, $Q^2 > 4\,\text{GeV}^2$ and inelasticity $0.05 < y < 0.7$.

2. Muons were identified by requiring the presence of a reconstructed track segment in the forward, barrel or rear muon chambers, or by a segment or energy deposit in the backing calorimeter [11]. These segments or deposits were matched in space to a corresponding track in the CTD, from which the muon momentum measurement was obtained. In the forward region, this momentum was combined with the momentum measured in the FMUON, if available. If the muons are sufficiently isolated in the calorimeter, their muonic nature was confirmed by the detection of a minimum ionising energy deposit (mip) in the main ZEUS calorimeter. This redundant muon selection yields an efficiency of about 80% per muon for high momentum muons. Cuts on the muon transverse momentum $p_T^\mu > 1.5\,\text{GeV}$ and on pseudorapidity $\eta^\mu > -1.6$ were applied.

   The reconstruction efficiency of the muon system was corrected separately for each detector component depending on p_T^μ and η^μ.

3. Hadronic final-state objects, reconstructed from tracks and energy deposits in the calorimeter were clustered into jets using the k_T cluster algorithm (KTCLUS) [17] in its massive mode with the E_T recombination scheme. Reconstructed muons were

included in the clustering procedure. Selected events contained at least one jet with $E_T^{\rm jet} > 5\,$GeV within the detector acceptance $-2 < \eta^{\rm jet} < 2.5$.

4. The muons were required to be associated to a jet using a cone of $R = \sqrt{\delta\phi^2 + \delta\eta^2} < 0.7$, where the associated jet was not necessarily the jet satisfying the cuts above. To ensure a good reconstruction of the associated jet, it was required to have transverse energy $E_T^{\rm jet} > 4\,$GeV.

After all selection cuts, the final data sample contained 4734 events. To correct the data for detector acceptance and to extract the beauty fraction, the RAPGAP 3 MC simulation [18] was used to generate signal (beauty) and background (charm) events. RAPGAP is a generator based on LO matrix elements, with higher-order QCD radiation simulated in the leading-logarithmic approximation. The hadronisation is simulated using the Lund string model as implemented in JETSET [19]. The background from light flavours is simulated using DJANGO [20]. It has been checked on a hadronic background sample of data and MC, that the MC reasonably well describes the shape of the $p_T^{\rm rel}$ distribution. The small differences are treated as a contribution to the systematic error.

3 Extraction of the b signal

The light flavour and charm quark MC samples were mixed according to their relative luminosities and the b-quark sample was added according to the beauty fraction determined from the $p_T^{\rm rel}$ analysis. Figure 1 shows the $p_T^{\rm rel}$ distribution as measured in the ZEUS detector for the data and MC distributions from beauty, charm and light flavours. The distribution peaks at low $p_T^{\rm rel}$, where the decays of hadrons containing charm and light quarks dominate. At higher $p_T^{\rm rel}$, the distribution falls less steeply than that expected for light and charm contributions alone. The data are consistent with a significant contribution from b quarks.

To determine the beauty fraction in the data, the contribution from light flavour plus charm, and beauty, were allowed to vary and fitted to the data using the χ^2 method. The measured beauty fraction is $f_{\rm beauty} = 21 \pm 2\%$(stat.). The sum of the MC contributions shown in Fig. 1 describes the data well. Figure 2 shows the comparison between the data and the MC simulation with respect to various variables of the measured muon and the associated jet. Here, the relative fractions of the contributions from beauty and light plus charm quarks have been fixed by the procedure described above. The MC agrees reasonably well with the measured distributions. This demonstrates that the RAPGAP MC can be reliably used to calculate the detector-acceptance corrections.

4 Results

Results in the DIS region for HERA I data have been previously measured by ZEUS [9]. After the upgrade to HERA II the beauty production measurement was performed in a wider kinematic range. Events were selected by requiring the presence of at least one muon and one jet in the final state. A total visible cross section of

$$\sigma_{b\bar{b}} = 77.1 \pm 7.8(\text{stat.}) \pm^{9.6}_{14.9} (\text{syst.})\,\text{pb}$$

was measured for the reaction $e^+p \rightarrow e^+b\bar{b}X \rightarrow e^+\mu$ jet X' in the kinematic region defined by: $Q^2 > 4\,\text{GeV}^2$, $0.05 < y < 0.7$, $p^\mu > 1.5\,\text{GeV}$, $\eta^\mu > -1.6$ and one jet with $E_T^{\text{jet}} > 5\,\text{GeV}$ and $-2 < \eta^{\text{jet}} < 2.5$ associated to the muon. The systematic uncertainty is the quadratic sum of different individual uncertainties coming from the muon-efficiency correction, p_T^{rel} shape for light flavours, ratio of light flavours to charm, energy scale and luminosity uncertainty. This result was compared to a NLO QCD calculation from HVQDIS [21], after folding the b-quark momentum spectrum with a Peterson fragmentation function and subsequently with a spectrum of the semi-leptonic muon momentum extracted from Rapgap [18]. A mixture of direct ($b \rightarrow \mu$) and indirect ($b \rightarrow c \rightarrow \mu$) b-hadron decays to muons has been used. The b quark mass was set to $m_b = 4.75\,\text{GeV}$ and the renormalisation and factorisation scales to $\mu = \sqrt{p_T^2 + 4m_b^2}$. The CTEQ5F4 parton densities [22] have been used. The cross section was determined using the sum of the branching ratios of direct and indirect decays of b hadrons into muons, which was fixed to 0.22, as implemented in Jetset. The NLO QCD prediction is

$$\sigma_{\text{NLO}} = 32.9 \pm 3.3\,\text{pb},$$

where the error has been estimated by varying the scale μ by a factor of 2 and 1/2 and the mass m_b between 4.5 and 5.0 GeV. The measured total cross section is about 2σ higher than the NLO prediction. The differential cross sections were measured in the same kinematic range as the total visible cross section by repeating the fit of the p_T^{rel} distribution in each bin. Figure 3 shows differential cross section as a function of Q^2 compared to the NLO calculation and the LO QCD plus PS Rapgap MC predictions scaled to the data. Differential cross sections as functions of p_T^μ (Fig. 4), η^μ (Fig. 5), p_T^{jet} (Fig. 6) and η^{jet} (Fig. 7) are also shown. In all distribution the data are described in shape by the MC and by the NLO QCD calculation. The constant factor between the data and the NLO QCD calculations in these distributions reflects the 2σ difference seen in the total cross section. Double-differential cross sections, $d^2\sigma/dxdQ^2$, were also measured (see Fig. 8). They can be used as input to calculate the beauty contribution to the proton structure function F_2.

5 Conclusions

The production of beauty quarks in the deep inelastic scattering (DIS) process $e^+p \rightarrow e^+b\bar{b}X \rightarrow e^+\mu$ jet X' has been measured with the ZEUS detector at HERA II. The total visible cross section is 2σ higher than the NLO prediction. Differential cross sections $d\sigma/dQ^2$, $d\sigma/dp_T^\mu$, $d\sigma/d\eta^\mu$, $d\sigma/dp_T^{\mathrm{jet}}$ and $d\sigma/d\eta^{\mathrm{jet}}$ were measured. In all distribution the data are described in shape by the MC and by the NLO QCD calculation. Double-differential cross sections in x and Q^2 have been measured to allow the calculation of the beauty contribution to the proton structure function F_2.

References

[1] CDF Coll., F. Abe et al., Phys. Rev. **D 55**, 2546 (1997).

[2] DØ Coll., B. Abbott et al., Phys. Lett. **B 487**, 264 (2000).

[3] CDF Coll., D. Acosta et al., Phys. Rev. **D 71**, 032001 (2005).

[4] H1 Coll., A. Aktas et al., Eur. Phys. J. **C 41**, 453 (2005).

[5] H1 Coll., A. Aktas et al., Phys. Lett. **B 621**, 56 (2005).

[6] H1 Coll., A. Aktas et al., Eur. Phys. J. **C 40**, 349 (2005).

[7] H1 Coll., A. Aktas et al., Eur. Phys. J. **C 45**, 23 (2006).

[8] ZEUS Coll., S. Chekanov et al., Phys. Rev. **D 70**, 12008 (2004).

[9] ZEUS Coll., S. Chekanov et al., Phys. Lett. **B 599**, 173 (2004).

[10] ZEUS Coll., J. Breitweg et al., Eur. Phys. J. **C 18**, 625 (2001).

[11] ZEUS Coll., U. Holm (ed.), *The ZEUS Detector*. Status Report (unpublished), DESY (1993), available on `http://www-zeus.desy.de/bluebook/bluebook.html`.

[12] M. Derrick et al., Nucl. Inst. Meth. **A 309**, 77 (1991);
A. Andresen et al., Nucl. Inst. Meth. **A 309**, 101 (1991);
A. Caldwell et al., Nucl. Inst. Meth. **A 321**, 356 (1992);
A. Bernstein et al., Nucl. Inst. Meth. **A 336**, 23 (1993).

[13] N. Harnew et al., Nucl. Inst. Meth. **A 279**, 290 (1989);
B. Foster et al., Nucl. Phys. Proc. Suppl. **B 32**, 181 (1993);
B. Foster et al., Nucl. Inst. Meth. **A 338**, 254 (1994).

[14] ZEUS Coll., *A Microvertex Detector for ZEUS*, Proposal DESY PRC 97/01, DESY, 1997. Also as internal ZEUS Note ZEUS-97-006.

[15] M. Bobrowski et al., Nucl. Inst. Meth. **A 323**, 309 (1992).

[16] J. Andruszków et al., Acta Phys. Pol. **B 32**, 2025 (2001).

[17] S.D. Ellis and D.E. Soper, Phys. Rev. **D 48**, 3160 (1993).

[18] H. Jung, Comp. Phys. Comm. **86**, 147 (1995).

[19] T. Sjöstrand, Comp. Phys. Comm. **82**, 74 (1994).

[20] G.A. Schuler and H. Spiesberger, *Proc. Workshop on Physics at HERA*, W. Buchmüller and G. Ingelman (eds.), Vol. 3, p. 1419. Hamburg, Germany, DESY (1991).

[21] B.W. Harris and J. Smith, Phys. Rev. **D 57**, 2806 (1998).

[22] CTEQ Coll., H.L. Lai et al., Eur. Phys. J. **C 12**, 375 (2000).

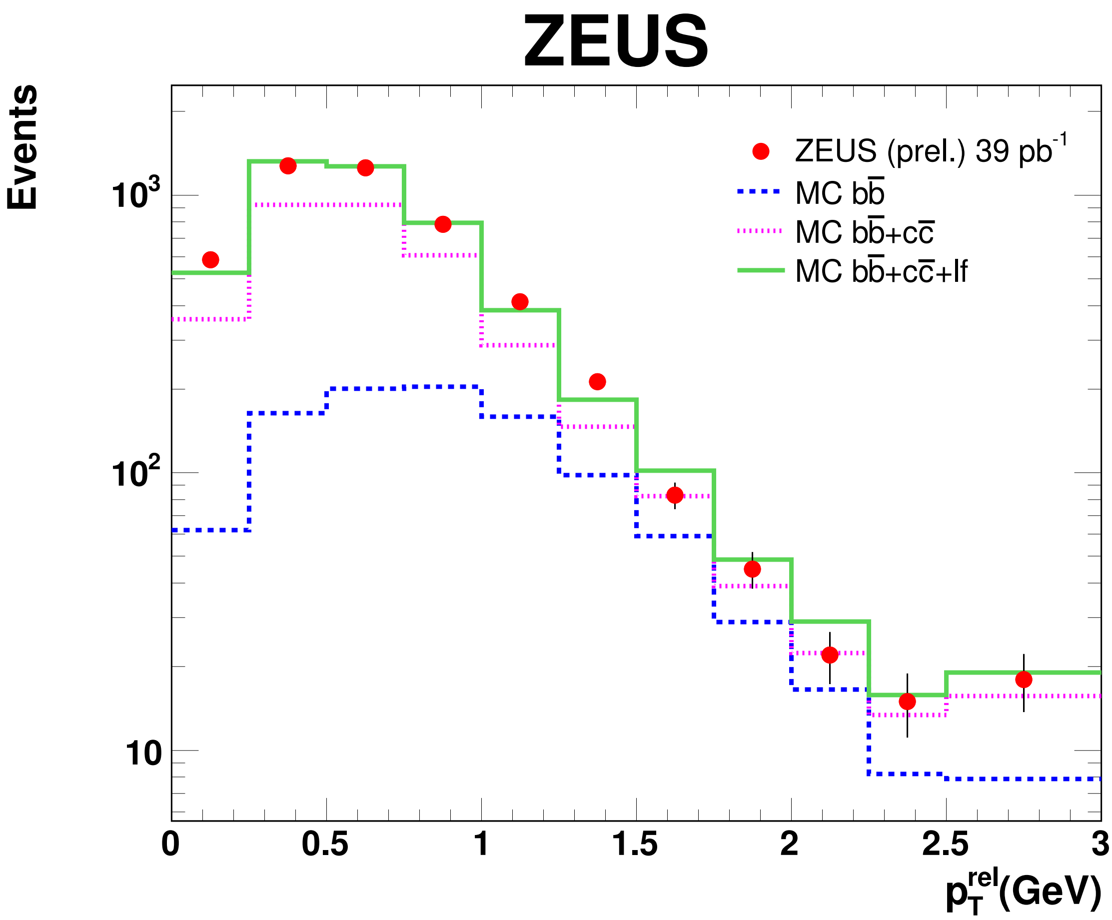

Figure 1: *Measured p_T^{rel} distribution for the data and MC. The fitted contribution from beauty quarks is shown as dashed histogram. Adding the contributions of charm (dotted histogram) and light flavour gives the sum of all MC (solid histogram). The data points are plotted with statistical errors only.*

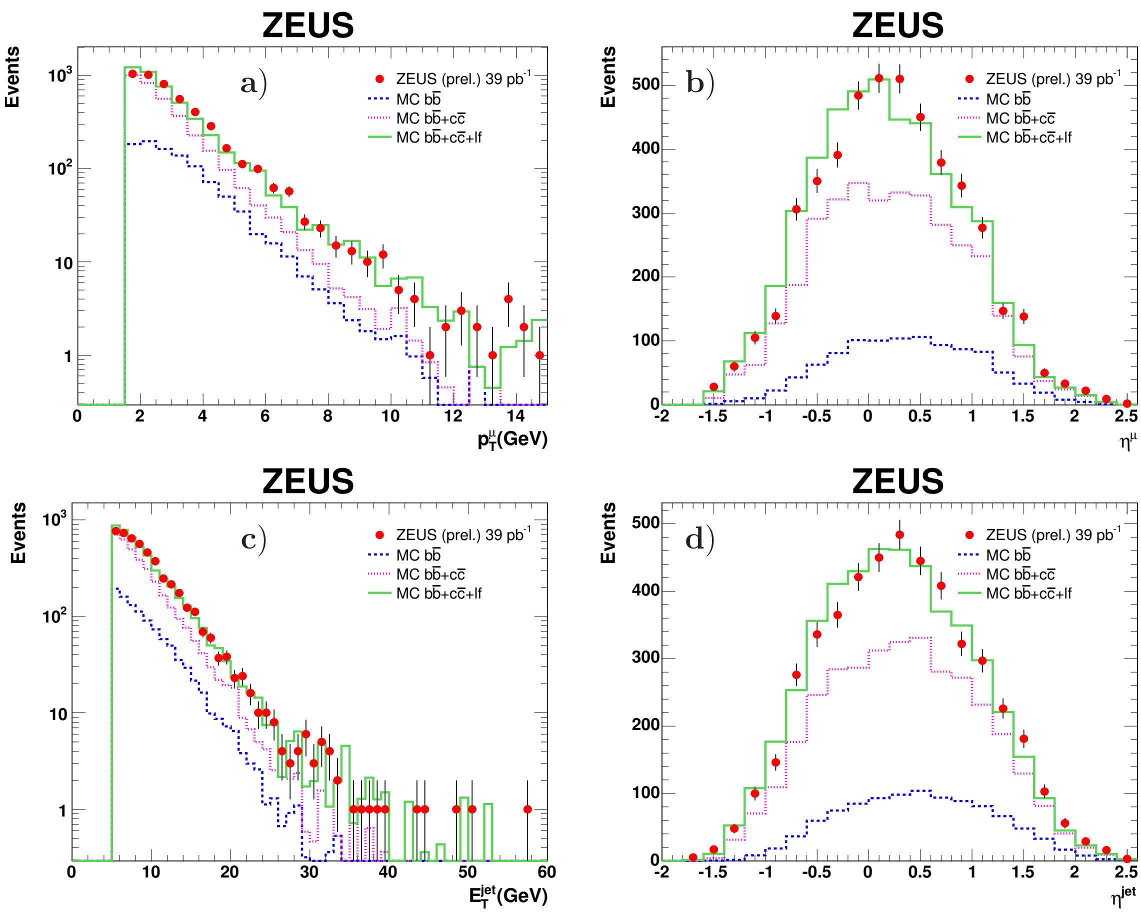

Figure 2: *Control distributions for data (dots) and MC (*Rapgap*) using the p_T^{rel}-fit after final cuts. The distribution of the transverse momentum of the muon (a), pseudorapidity of the muon (b), transverse energy of the jet (c) and pseudorapidity of the jet (d) are shown. The data points are plotted with statistical errors only.*

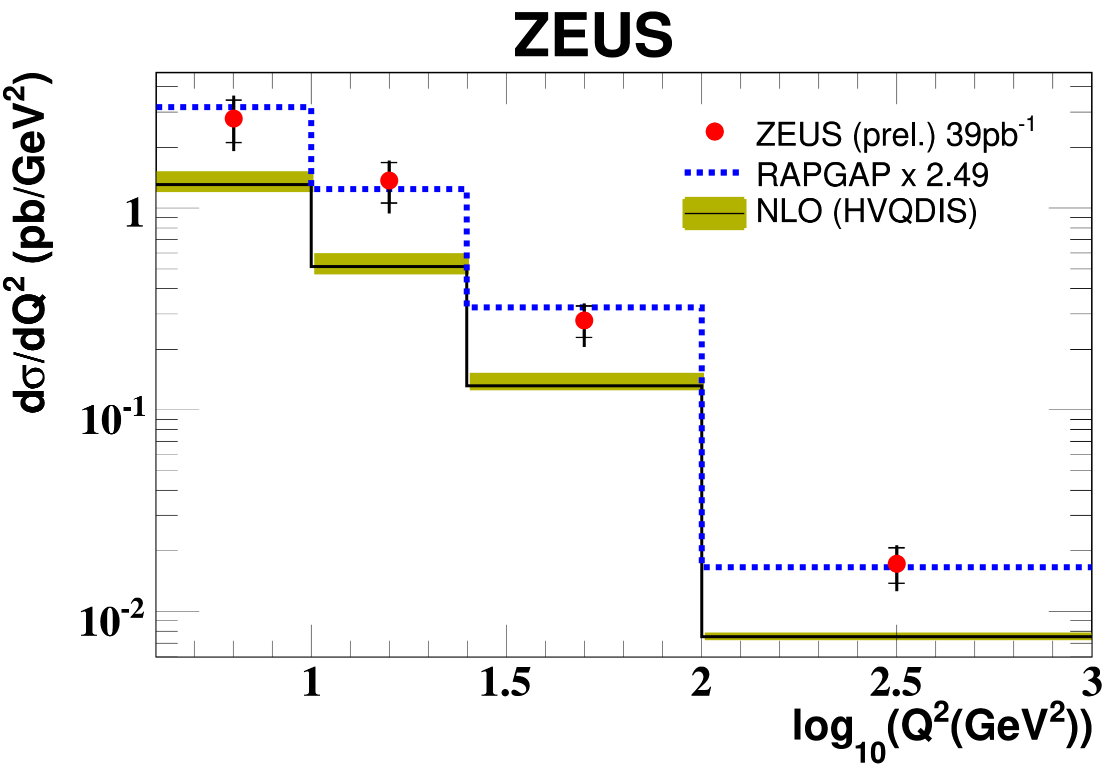

Figure 3: *Differential beauty cross section as a function of the photon virtuality Q^2 for events with at least one jet and one muon, compared to* RAPGAP *MC (LO QCD with DGLAP evolution) normalised to the data and to NLO QCD calculations. The errors on the data points correspond to the statistical uncertainty (inner error bars) and to the statistical and systematical uncertainty added in quadrature (outer error bars). The shaded bands show the uncertainty of the theoretical prediction coming from the variation of the renormalisation and factorisation scale, μ, and the b-quark mass, m_b.*

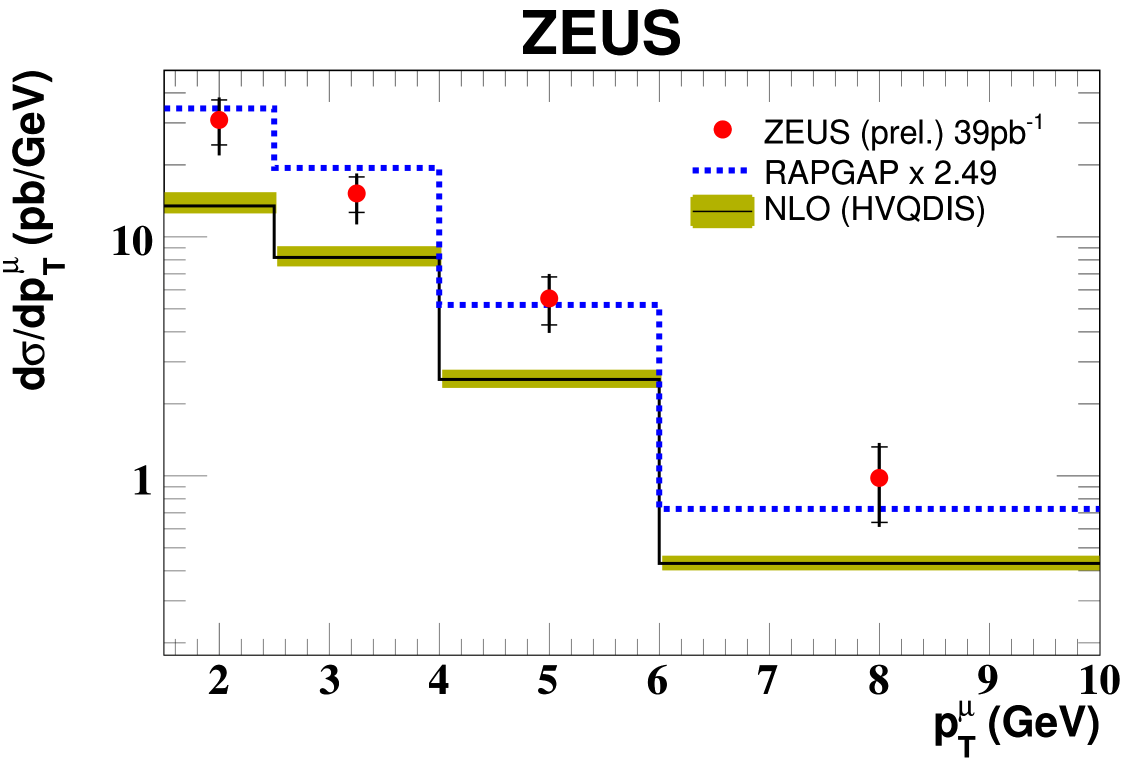

Figure 4: *Differential beauty cross section as a function of p_T^μ compared with the NLO QCD calculations and scaled MC.*

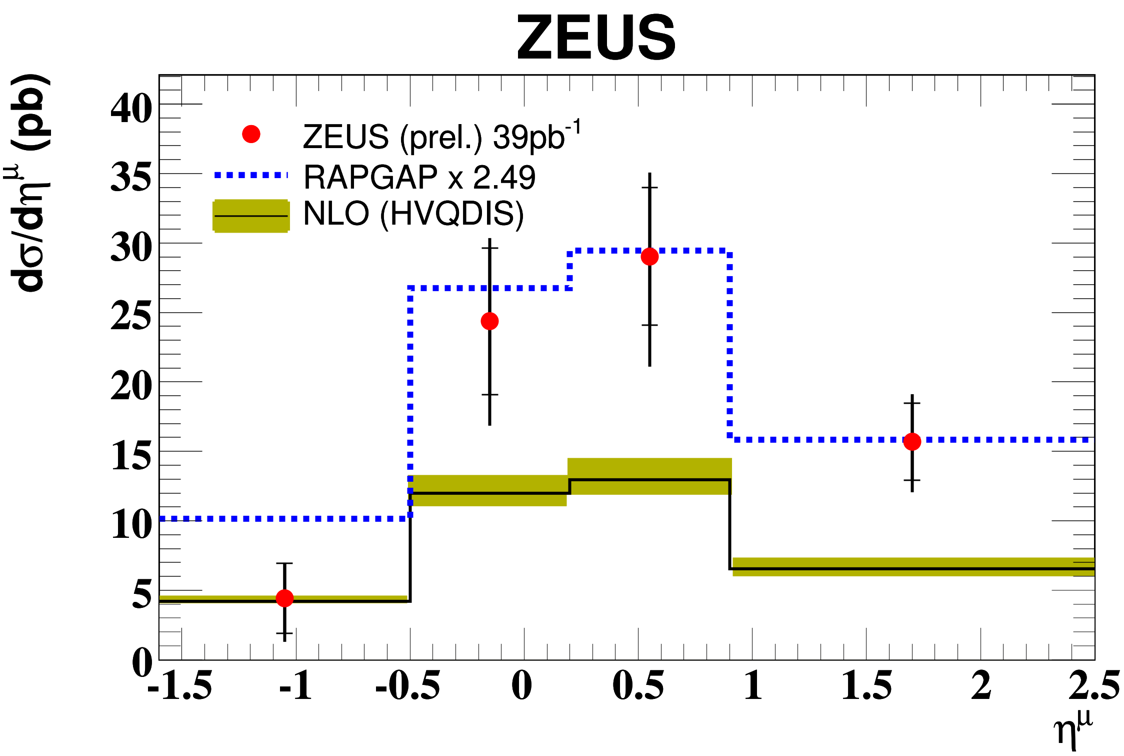

Figure 5: *Differential beauty cross section as a function of η^{μ} compared with the NLO QCD calculations and scaled MC.*

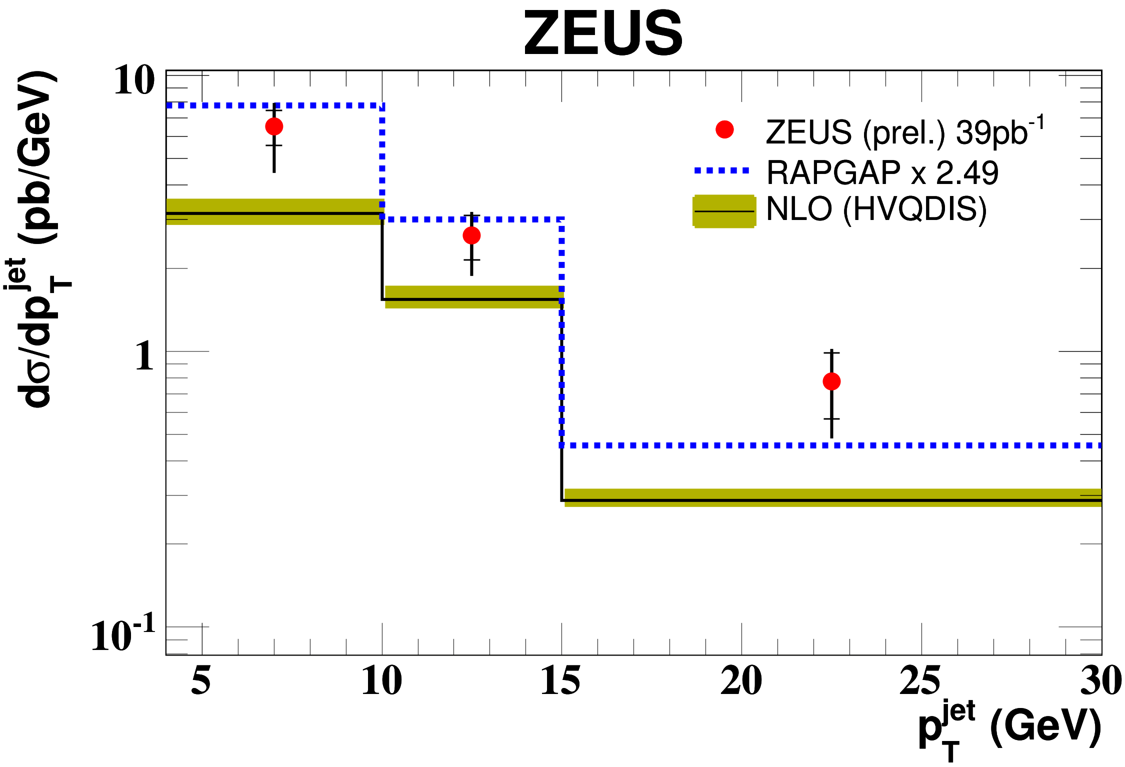

Figure 6: *Differential beauty cross section as a function of $p_T^{\rm jet}$ compared with the NLO QCD calculations and scaled MC.*

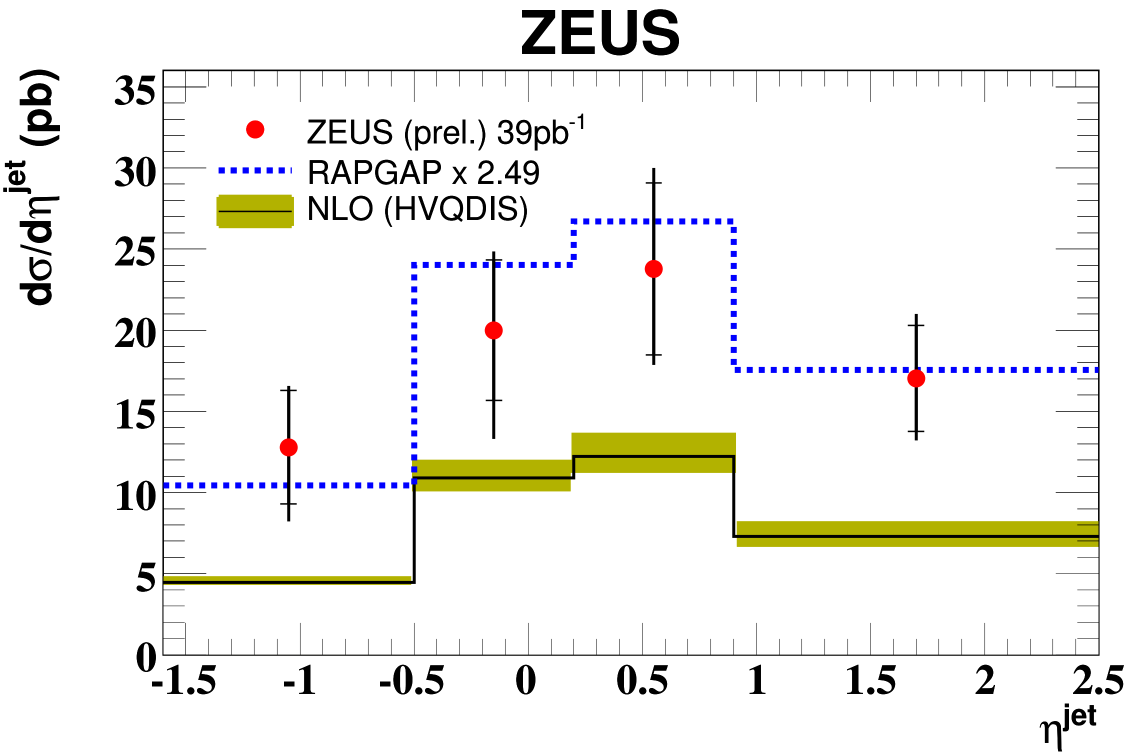

Figure 7: *Differential beauty cross section as a function of* $\eta^{\rm jet}$ *compared with the NLO QCD calculations and scaled MC.*

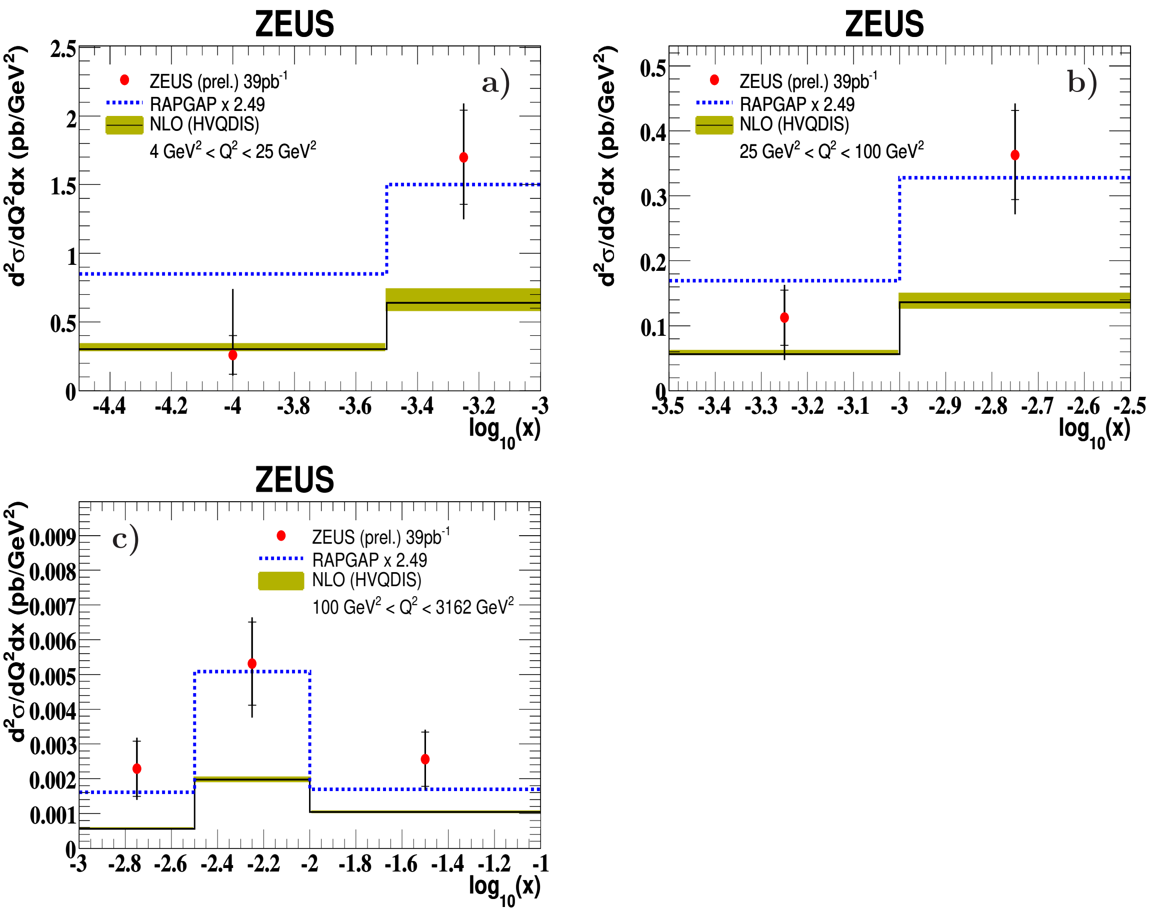

Figure 8: *Double-differential beauty cross section as a function of Bjørken x and Q^2 for $4 < Q^2 < 25$ GeV^2 (a), $25 < Q^2 < 100$ GeV^2 (b) and 100 $GeV^2 < Q^2$ (c) compared with the NLO QCD calculations and scaled MC.*